Taylor & Francis
Taylor & Francis Group

A collective model for inner shell ionization of very heavy targets

C.C. Montanari[a,b]*, D.M. Mitnik[a,b] and J.E. Miraglia[a,b]

[a]*Instituto de Astronomía y Física del Espacio, Casilla de Correo 67, Sucursal 28, C1428EGA Buenos Aires, Argentina;* [b]*Departamento de Física, Facultad de Ciencias Exactas y Naturales, Universidad de Buenos Aires, Buenos Aires, Argentina*

We present a theoretical study of the ionization of inner shells, such as L and M shells of Au, Pb and Bi or K-shell of Sb. The ionization is described using a collective response model, the shellwise local plasma approximation (SLPA). This model deals with each sub-shell of target electrons as an inhomogeneous electron gas with an ionization threshold. No parameters are included, just the theoretical wave functions of the ground state and the binding energies. The validity range is that of the perturbative approximation, high energies and asymmetric projectile target relation. In the case of Sb, known Hartree–Fock wave functions and energies are used. Instead, for Au, Pb and Bi, they were obtained in fully relativistic way by solving numerically the Dirac equation. The SLPA describes well the experimental data for K-shell ionization of Sb by O and F positive ions. However, it underestimates the data for C or lighter ions. Good results are obtained for M-shell ionization of Au and Bi above 2 MeV/amu, and for L-shell ionization of Au and Pb above 10 MeV/amu. For L- and M-shells, the SLPA tends to underestimate the data for energies below the range of validity of the model but approaches the experimental data for higher energies.

Keywords: ionization; inner-shells; ions, electrons

1. Introduction

Ionization of different shells has attracted great attention over recent decades, especially regarding the characteristic radiation from inner shells and the characterization of materials. For K- and L-shell ionization, important compilations of data are available (*1*, *2*) and are in continuous revision (*3–5*), together with fittings and suggested reference cross-sections (*6*, *7*). Reliable ionization cross-sections are sensitive and critical inputs for particle-induced X-ray emission (PIXE) analysis (*8*). One of the most employed theories is the ECPSSR of Brandt and Lapicki (*9*) and its evolutions (*10*) of probed efficacy, which covers an extended energy range and is the usual input in PIXE codes.

On the other hand, the choice of atomic parameters (multiple ionization probabilities, fluorescence yields) for the conversion of the experimental X-ray production cross-sections to sub-shell ionization cross-sections is still a subject of discussion (*4*, *5*, *11*). This is not a minor problem, and

shows that the question about reliable values of ionization cross-sections of different sub-shells is still an open subject.

From a theoretical point of view, the inner-shell ionization is an important challenge with which to test the capability of a theory to describe wave functions and interaction potentials. Different approaches have been employed over the years, most of them within the independent electron model (from the distorted wave methods up to the numerical solution of the Schrödinger equation). However, ionization of deep shells represents a task for first principle models, especially for very heavy targets which include N- or O-shells.

The goal of this work is to present calculations for these deep shells using a collective description known as shellwise local plasma approximation (SLPA) (*12*). It works within the dielectric formalism (not the independent electron model or hydrogenic potentials). Instead, each sub-shell is described as a whole, including screening and correlation among electrons. The SLPA starting points are the atomic density of electrons of a certain sub-shell and the corresponding binding energy. We have a particular interest in testing the SLPA description for the ionization of Au, Pb and Bi in relation to recent stopping power calculations (*13*), where we found a systematic overestimation in the high-energy region (2–10 MeV/amu) (*14*).

The present contribution involves the calculation of ionization cross-sections in the energy region of a few MeV/amu up to some tens of MeV/amu, depending on the shell. We first test the model for Sb, which implies the calculation with tabulated Hartree–Fock wave functions and binding energies. Then we apply the same formalism for Au, Pb and Bi, using fully relativistic wave functions and binding energies calculated in a recent paper (*13*). Results for K-, L- or M-shell ionization for these targets and different ions are presented and compared with experimental ionization cross-sections and the ECPSSR results, when available.

2. Theoretical calculations

2.1. *The relativistic binding energies and densities*

The fully relativistic wave functions were generated by using the GRASP code (*15*, *16*). The theoretical framework of this code is the first-order perturbation theory with a central field. The zero-order wave functions are solutions of the Dirac equation. The Hamiltonian is diagonalized on the basis of these wave functions (configuration interaction). The first-order perturbation theory contribution from the Breit interaction energies is also included in the calculations, as well as QED corrections. The binding energies are calculated using the fully relativistic multi-configurational RELAC code (*17*), based on the parametric potential model (*18*). A more detailed explanation of these calculations can be found in (*13*).

We display the theoretical results for the K, L and M binding energies in Table 1, together with experimental binding energies in solids. The agreement between the theoretical results and the experimental data is good, with a difference of around 1% for the L-shell and 2% for the M-shell. In all the cases, the theoretical results are above the experimental values.

2.2. *The SLPA*

The SLPA is a general method with which to calculate the contribution of the ionization of target-bound electrons to the different moments of the energy loss (cross-sections (*20–22*), stopping power (*23*, *24*), straggling (*25*)). It considers explicitly the ionization gap and only describes together the electrons with the same binding energy. It is based on the local plasma approximation by Lindhard and Scharff (*26*) and has been extensively used since then in stopping power calculations (*27*). However, the present formulation has important differences, as explained below.

Table 1. Binding energies for K-, L- and M-shells of neutral Au, Pb and Bi.

nlj	Au		Pb		Bi	
	E^{exp}	E^{th}	E^{exp}	E^{th}	E^{exp}	E^{th}
K						
1s	2966	2988	3234	3258	3327	3352
L						
2s	527.5	532.4	582.9	588.2	602.3	607.8
2p1/2	504.7	509.3	558.6	563.5	577.4	582.5
2p3/2	438.0	441.7	479.0	482.9	493.2	497.1
M						
3s	125.9	128.1	141.5	143.8	147.0	149.4
3p1/2	115.7	117.8	130.6	132.8	135.8	138.1
3p3/2	100.8	102.7	112.7	114.6	116.8	118.7
3d3/2	84.20	85.95	95.03	96.81	98.79	100.6
3d5/2	81.07	82.74	91.29	92.97	94.82	96.55

Notes: E^{exp} are the experimental values as compiled by Williams (*19*). E^{th} are the fully relativistic binding energies, calculated by using the GRASP code (*18*). Atomic units are used.

The ionization cross-section of the *nl*-subshell electrons due to the interaction with an ion of impact velocity v, nuclear charge Z_{P}, N bound electrons and charge state $q = Z_{\mathrm{P}} - N$ is expressed as:

$$S_q^{nl} = \frac{2}{\pi v^2} \int_0^\infty \frac{\mathrm{d}k}{k} [Z_q(k)]^2 \int_0^{kv} \mathrm{d}\omega \int \mathrm{d}\vec{r} \, \mathrm{Im}\left[\frac{-1}{\varepsilon_{nl}(k, \omega, \delta_{nl}(r), E_{nl})} \right], \tag{1}$$

with $Z_q(k)$ being the effective ion charge considering bound electrons as frozen (just screening the nucleus). Using Flannery integrals (*28*), it has a simple closed form if a Slater-type expansion is used to represent the wave functions (see Appendix).

As expected, $Z_q(k)$ tends to the nuclear charge Z_{P} for close collisions (large k) and to $q = Z_{\mathrm{P}} - N$ for long distance collisions ($k \to 0$).

The ionization gap or binding energy of each sub-shell, E_{nl}, is introduced explicitly in Equation (1) by using the Levine–Louie dielectric response (*29*). This dielectric function keeps the f-sum rules and properties of the Lindhard one (*30*) (electron–electron correlation, screening among electrons of the same shell and collective response, if any). It is a linear response (first order in the projectile charge), so this SLPA works within the perturbative limit.

We employ Equation (1) to calculate ionization cross-sections of Sb with local densities of electrons, $\delta_{nl}(r)$, and binding energies, E_{nl}, from known Hartree–Fock calculations (*31*). Instead, for Au, Pb and Bi, we use the relativistic solutions of the Dirac equation mentioned in the previous section, with the theoretical binding energies, E^{th}, displayed in Table 1.

3. Results

The SLPA has the advantage of describing deep shells with the same difficulty as the outer shell. We first test the model for K-shell ionization of Sb ($Z = 51$) by C^{+q}, O^{+q} and F^{+q} ions with different charge states. In Figure 1, we show the results in the energy range of a few MeV/amu. In fact, the SLPA is expected to describe the data for much higher energies ($E > 20\,\mathrm{MeV/amu}$), but the comparison of the present results with the ECPSSR and with the experimental data is quite good, especially for O and F ions. However, it underestimates the data for C ions by a factor of 2.
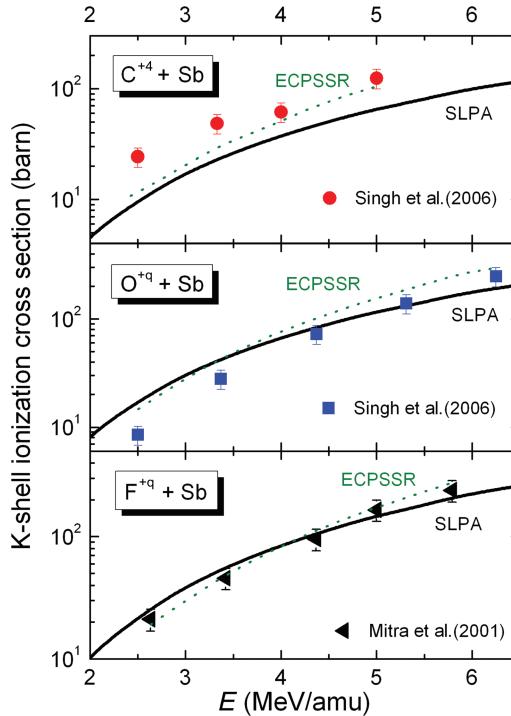
Figure 1. K-shell ionization of Sb by C^{+4}, O^{+q} and F^{+q} ions. Solid lines, present SLPA calculations; dotted lines, ECPSSR results. Experimental data by Tribedi and collaborators for C and O ions (*32*) and F ions (*33*).

Though theoretical calculations were performed for different ion charge states using the screened ion charge $Z_q(k)$ given by Equation (A3), we obtain similar results for F^{+9} or F^0. In fact, both experimental and theoretical values show no dependence on the number of bound electrons in the ion. This result is not surprising; the K-shell of Sb has a mean radius of $\langle r_K \rangle \approx 0.03$ a.u. (*31*), while the radius of the K-shell of F^0 is 0.18 a.u., six times larger. Regardless of the number of electrons carrying the fluorine projectile, the ionization of the K-shell of Sb is governed by the interaction with the ion nucleus. In the perturbative region, this means a Z_P^2 dependence.

In Figure 2, we plot the scaling of the ionization cross-sections with Z_P^2, including data for H^+ and He^{+2}. We can observe that the data for the O^{+q} and F^{+q} ions follow a certain tendency, while the results for H^+, He^{+2} and C^{+4} ions seem to follow a different one. The SLPA is a single curve (the same for protons or F^{+q}), which surprisingly describes the heaviest ions better than the lightest ions. These unexpected results open two fronts. From a theoretical point of view, the SLPA for K-shell ionization by different ions needs further research. In experimental terms, we should return to the discussion about the parameters for the conversion from measured X-ray cross-sections to ionization cross-sections.

In Figures 3 and 4, we present the main results of this work. The SLPA is expected to describe L-shell ionization of Au, Bi or Pb for $E > 20$ MeV/amu and M-shell ionization for $E > 4$ MeV/amu. For these very heavy targets, the description of K-shell ionization with the SLPA needs relativistic impact velocities ($v > 54$).

The comparison of the ionization cross-sections with the experimental data is good for $E > 15$ MeV/amu for L-shell ionization of Au and Pb. This is an interesting result for a very deep shell calculated fully theoretically. In the case of M-shell ionization of Au and Bi, the SLPA results are good for $E > 2$ MeV/amu, better for Bi than for Au, when compared with recent
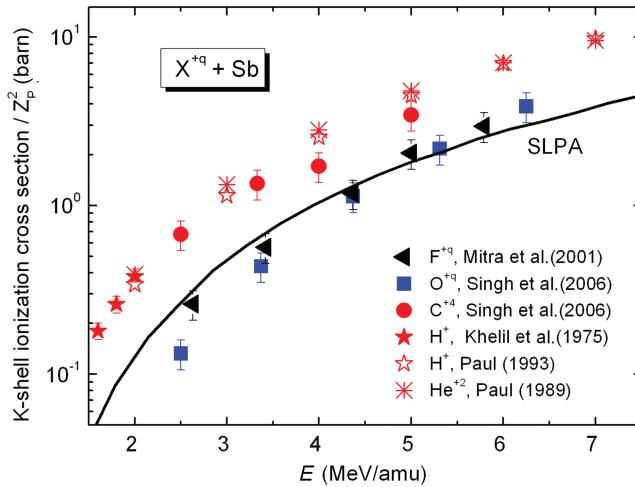
Figure 2. Scaled K-shell ionization cross-section of Sb by different ions. Experimental data for C, O and F ions as in Figure 1. Proton ions, solid stars (*34*), hollow stars (*6*); He^{2+} ions, asterisks, data by Paul and Bolik (*7*).

measurements by Czarnota et al. (*36*). Again the mean radius for target electrons is small when compared with the radius of K-electrons in the projectile, and the theoretical results, calculated considering the bound electrons in the projectile are the same of those for the bare ions. In all cases, the SLPA tends to underestimate the experimental values and is below the ECPSSR curve,
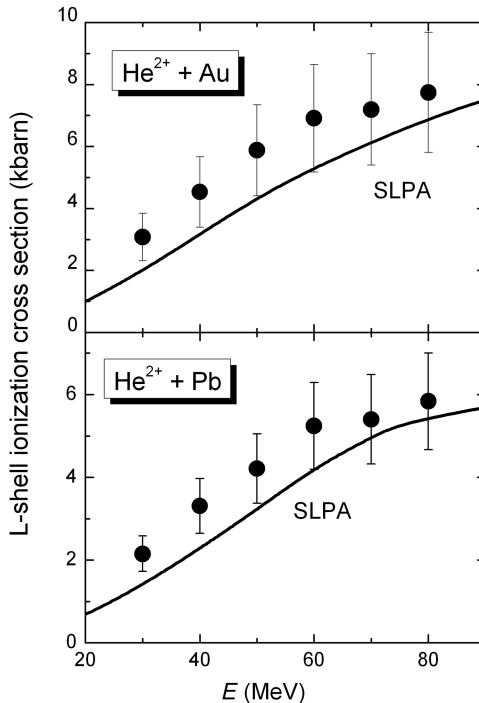

Figure 3. L-shell ionization of Au and Pb by He^{+2}. Solid lines present SLPA calculations. Experimental data by Hardt and Watson (*35*).
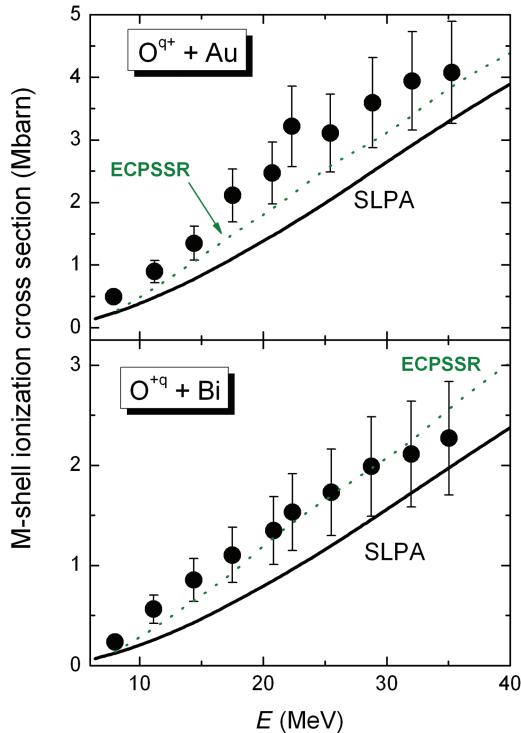
Figure 4. M-shell ionization of Au and Bi by O^{+q} ions, with q = 3–6. Solid lines present SLPA calculations. Dotted lines, ECPSSR results. Experimental data by Czarnota et al. (*36*).

which describes the M-shell ionization as very good. Note that for both L- and M-shell ionization, these energies are below the energy range, so the SLPA is expected to work.

4.   Concluding remarks

We present theoretical calculations for K-, L- and/or M-shell ionization cross-sections of certain heavy targets ($Z = 51, 79, 82$ and 83) using the SLPA. The results are very good for K-shell ionization of Sb by F and O in the MeV/amu energy range, but not for H, He or C ions. For L- and M-shell ionization of Au, Pb and Bi, the impact energies should be higher than 15 MeV/amu (L-shell) and 2 MeV/amu (M-shell). The SLPA shows a tendency to underestimate the cross-sections for impact velocities below that of the target electrons.

The collective description performed using the SLPA is a useful alternative model, especially for these very heavy ions. It is simple to calculate and only requires the density and binding energies of target electrons. Extension to more complex systems is straightforward. On the other hand, the comparison with the known ECPSSR formalism is good, taking into account the *ab initio* calculation in the SLPA. Some theoretical and experimental doubts are presented about K-shell ionization cross-sections, however, which show that this subject, despite having been studied over many years and with lots of compilations and useful codes, is still open to analysis.

Acknowledgements

References

(1) Rosato, E. *Nucl. Instrum. Methods A* **1989,** *280,* 365–369; *Nucl. Instrum. Methods B* **1991,** *56/57,* 38–40.
(2) Orlic, I.; Sow, C.H.; Tang, S.M. *At. Data Nucl. Data Tables* **1994,** *56,* 159–210.
(3) Lapicki, G. *X-Ray Spectrom.* **2005,** *34,* 269–278; **2009,** *42,* 145204.
(4) Lapicki, G.; Miranda, J. *J. Phys.: Conf. Series* **2009,** *194,* 082008.
(5) Lapicki, G.; Miranda, J. In 21st International Conference on the Application of Accelerators in Research and Industry (CAARI) 2010 Proceedings, THU-IBA07-2, 2010.
(6) Paul, H.; Sacher, J. *At. Data Nucl. Data Tables* **1989,** *42,* 105–156.
(7) Paul, H.; Bolik, O. *At. Data Nucl. Data Tables* **1993,** *54,* 75–131.
(8) Lapicki, G. *J. Phys. B: At. Mol. Opt. Phys.* **2009,** *42,* 145204-1–10.
(9) Brandt, W.; Lapicki, G. *Phys. Rev. A* **1979,** *20,* 465; *Phys. Rev. A* **1981,** *23,* 1717–1729.
(10) Lapicki, G. *Nucl. Instrum. Methods B* **2002,** *189,* 8–20.
(11) Dingfelder, M.; Fernández-Varea, J.M.; Segui, S. *J. Phys.: Conf. Series* **2009,** *194,* 042001.
(12) Montanari, C.C.; Miraglia, J.E. *Phys. Rev. A* **2006,** *73,* 024901.
(13) Montanari, C.C.; Archubi, C.D.; Mitnik, D.; Miraglia, J.E. *Phys. Rev. A 79,* **2009,** 032903.
(14) Montanari, C.C.; Mitnik, D.; Archubi, C.D.; Miraglia, J.E. *Phys. Rev. A* **2009,** *80,* 012901.
(15) Grant, I.P. et al. *Comput. Phys. Commun.* **1980,** *21,* 207–231.
(16) McKenzie, J. et al. *Comput. Phys. Commun.* **1980,** *21,* 233–246.
(17) Klapisch, M.; Schwob, J.L.; Frankel, B.S.; Oreg, J. *J. Opt. Soc. Am.* **1977,** *67,* 148–155.
(18) Klapisch, M. *Comput. Phys. Commun.* **1971,** *2,* 239–260.
(19) Williams, G.P. *Electron Binding Energies of the Elements, CRC Handbook of Chemistry and Physics,* 66th Ed. F170; 1986. http://www.jlab.org/~gwyn/ebindene.html.
(20) Miraglia, J.E.; Gravielle, M.S. *Phys. Rev. A* **2010,** *81,* 042709.
(21) Montanari, C.C.; Miraglia, J.E.; Arista, N.R. *Phys. Rev. A* **2002,** *66,* 042902.
(22) Kadhane, Montanari, C.C.; Tribedi, L.C. *Phys. Rev. A* **2003,** *67,* 032703; *J. Phys. B* **2003,** *36,* 3043–3054; *Radiat. Phys. Chem.* **2006,** *75,* 1542–1546.
(23) Cantero, E.D.; Fadanelli, R.C.; Montanari, C.C.; Behar, M.; Eckardt, J.C.; Lantschner, G.H.; Miraglia, J.E.; Arista, N.R. *Phys. Rev. A* **2009,** *79,* 042904.
(24) Montanari, C.C.; Miraglia, J.E. 2009, arXiv:0904.1386v1 [physics.atom-ph].
(25) Montanari, C.C.; Miraglia, J.E.; Heredia-Avalos, S.; Garcia-Molina, R.; Abril, I. *Phys. Rev. A* **2007,** *75,* 022903.
(26) Lindhard, J.; Scharff, M. *K. Dan. Vidensk. Selsk. Mat. Fys. Medd*. **1953,** *27,* 1–31.
(27) Bonderup, E.; *K. Dan. Vidensk. Selsk. Mat. Fys. Medd.* **1967,** *35,* 1–20; Chu, W.K.; Powers, D. *Rev. Lett A* **1972,** *40,* 23–24; Johnson, R.E.; Inokuti, M. *Comm. At. Mol. Phys.* **1983,** *14,* 19–31.
(28) Flannery, M.R.; Levy, H. *J. Chem. Phys.* **1969,** *50,* 2938–2940.
(29) Levine, Z.H.; Louie, S.G. *Phys. Rev. B* **1982,** *25,* 6310–6316.
(30) Lindhard, J.; *K. Dan. Vidensk. Selsk. Mat. Fys. Medd.* **1954,** *28,* 1–57.
(31) Clementi, E.; Roetti, C. *At. Data Nucl. Data Tables* **1974,** *14,* 177–478.
(32) Singh, Y.P.; Kumar, A.; Kadhane, U.; Tribedi, L.C. *Phys. Rev. A* **2006,** *74,* 052714.
(33) Mitra, D.; Singh, Y.; Tribedi, L.C.; Tandon, P.N.; Trautmann, D. *Phys. Rev. A* **2001,** *64,* 012718.
(34) Kelhil, N.A.; Gray, T.J. *Phys. Rev. A* **1975,** *11,* 893–900.
(35) Hardt, T.L.; Watson, R.L. *Phys. Rev. A* **1976,** *14,* 137–145.
(36) Czarnota, M.; Banás, D.; Braziewicz, J.; Semaniak, J.; Pajek, M.; Jaskóla, M.; Korman, A.; Traumann, D.; Kretschmer, W.; Lapicki, G. *Phys. Rev. A* **2009,** *79,* 032710.
(37) Reinhold, C.; Miraglia, J.E. *J. Phys. B* **1987,** *20,* 1069–1080.
(38) Montanari, C.C.; Miraglia, J.E.; Behar, M.; Duarte, P.F.; Arista, N.R.; Eckardt, J.C.; Lantschner, G.H. *Phys. Rev. A* **2008,** *77,* 042901.

Appendix. Analytical expression for the effective charge of neutral or positive ions using Hartree–Fock wave functions

The Fourier transform of the screened Coulomb potential can be expressed as (*37, 38*):

$$V(k) = -\frac{4\pi}{k^2} Z_q(k), \tag{A1}$$

with

$$Z_q(k) = Z_p - \sum_{j=1}^{N} <\varphi_j|e^{ik.r}|\varphi_j>, \tag{A2}$$

where $\varphi_j \equiv \varphi_{n_j l_j m_j}$ are the electronic wave functions of each electron j in the projectile ground state. Following (37), Equation (A2) can be rearranged as:

$$Z_q(k) = Z_p - \sum_{nl} N_{nl} Z_{nl}(k), \tag{A3}$$

where N_{nl} is the number of electrons in the nl-subshell and $Z_{nl}(k)$ is:

$$Z_{nl}(k) = \frac{1}{2l+1} \sum_m < \varphi_{nlm} | e^{i\vec{k}\cdot\vec{r}} | \varphi_{nlm} > . \tag{A4}$$

By using the Hartree–Fock wave functions for neutrals or for positive ions tabulated by Clementi and Roetti (31), we can express the electronic wave functions as:

$$\varphi_{nlm}(\vec{r}) = \sum_p C_{nlp} \chi_{plm}(r, \theta, \phi), \tag{A5}$$

with C_{nlp} being the tabulated coefficients and $\chi_{plm}(\theta, \phi)$ being the Slater-type orbital with integer quantum numbers (31)

$$\chi_{plm}(r, \theta, \phi) = [(2\alpha_{lp})!]^{-1/2} (2\zeta_{lp})^{\alpha_{lp}+1/2} r^{\alpha_{lp}-1} e^{-\zeta_{lp} r} Y_{lm}(\theta, \phi). \tag{A6}$$

The values of the coefficients ζ_{lp} and α_{lp} and the total number of p-terms in the addition of Equation (A5) are given by the tabulated Roothan–Hartree–Fock expansion by Clementi and Roetti (31). Introducing Equations (A5) and (A6) in Equation (A4), we obtain the following expression:

$$Z_{nl}(k) = \frac{1}{4\pi} \sum_p \sum_s C_{nlp} C_{nls} \frac{(2\zeta_{lp})^{\alpha_{lp}+1/2}}{[(2\alpha_{lp})!]^{1/2}} \frac{(2\zeta_{ls})^{\alpha_{ls}+1/2}}{[(2\alpha_{ls})!]^{1/2}} I_{sp}(k), \tag{A7}$$

where

$$I_{sp}(k) = \int r^{\alpha_{lp}+\alpha_{ls}-2} e^{-(\zeta_{lp}+\zeta_{ls})r + i\vec{k}\cdot\vec{r}} d\vec{r} \tag{A8}$$

is the Flannery–Levy (28) integral, which has a simple analytic solution.